SIMULATION STUDY OF HEPS BOOSTER OPERATION AT LOWER INJECTION ENERGY*

A. Y. Wang†[1,2], J. Q. Wang[1,2], Y. M. Peng[1], C. Meng[1]
[1]Institute of High Energy Physics, Chinese Academy of Sciences, Beijing, China
[2]University of Chinese Academy of Sciences, Beijing, China

Abstract

This study investigates the feasibility of high-charge, low-energy 300 MeV linac-to-booster injection for the High Energy Photon Source (HEPS) injector. The primary aim is to enable klystron hot-standby operation for the HEPS linac, thereby enhancing its operational reliability. Energy ramping simulations for the booster were conducted using *elegant*. Both Gaussian and non-Gaussian bunches were tracked. Simulations and analysis indicate that, with a suitable initial RF voltage, Transverse Mode-Coupling Instability (TMCI) is the limiting factor for the beam transmission rate in the booster. By optimizing the chromaticity to enhance Landau damping, TMCI can be effectively suppressed, significantly improving beam transmission rate. Further reducing the injected bunch energy spread, or adjusting the working point, results in additional gains in the beam transmission rate. Through this synergistic optimization of multiple parameters, it looks feasible to achieve stable transport of beam with bunch charge exceeding 5 nC in the booster at the lower injection energy mode for the HEPS injector.

INTRODUCTION

The HEPS injector consists of a 500 MeV linac and a 6 GeV full-energy booster synchrotron [1]. Currently, the linac is equipped with five klystrons, which cannot provide a single-klystron hot-standby capability while still delivering a beam energy of 500 MeV. For the purpose to enable a klystron hot-standby for the HEPS linac, thereby improving the operational reliability of HEPS linac and reducing power consumption of HEPS, while also meeting the design requirement of at least 5 nC per bunch, this study investigates the feasibility of high-charge, low-energy linac-to-booster injection when the beam energy from the linac is reduced to 300 MeV [2].

Many synchrotron light sources worldwide have gained valuable experience in low-energy linac-to-booster injection under the condition that the beam energy from the linac is reduced. For example, ALBA achieved low-energy linac-to-booster injection when the injection energy was reduced from 110 MeV to 67 MeV through a fine quadrupole calibration and tuning of the quadrupoles at low excitation current and the compensation of the dipole eddy currents effect during booster ramping [3]. NSLS-II also successfully achieved low-energy linac-to-booster injection when the injection energy was reduced from 200 MeV to 115 MeV using beam-based online optimizations on the booster [4,5]. Beam dynamics simulations of TPS booster synchrotron showed the significant impact of magnet field errors and space charge effects on beam transmission rate when the injection energy was lowered from 150 MeV to 100 MeV [6].

However, due to the requirement to achieve low natural emittances together with high charge in the HEPS booster [1], new challenges arise in the HEPS injector during low-energy 300 MeV linac-to-booster injection, beyond those reported in the aforementioned experiments. In our study, we found that the main factors limiting the beam transmission rate for the booster can be attributed to two aspects. First, the high-charge requirement makes the TMCI highly prone to being triggered, leading to a significant degradation in beam transmission rate. Second, ignoring the effect of charge, when the linac operates at 300 MeV, the emittances and energy spread of the output beam increase by approximately 60% compared to operation at 500 MeV [2]. The larger energy spread and larger emittances may cause some particles to more easily trigger resonance, resulting in particle loss, further reducing the beam transmission rate.

The key parameters used in this study are shown in Table 1.

Table 1: Key Parameters of the HEPS Booster Used in This Study

Parameter	Symbol	Value and Unit
Circumference	C	454.07 m
Beam energy	E_0	300 MeV / 6 GeV
Betatron tunes	ν_x/ν_y	21.15 / 11.21
Momentum compaction factor	α_c	2.26×10^{-3}
Horizontal radiation damping time	τ_x	37.46 s / 4.68 ms
Vertical radiation damping time	τ_y	37.46 s / 4.68 ms
Longitudinal radiation damping time	τ_δ	18.73 s / 2.34 ms
Radiation energy loss per turn	U_0	24.26 eV / 3.88 MeV
Repetition rate	f_{rep}	1 Hz
RF frequency	f_{RF}	499.8 MHz
Harmonic number	h	757

SIMULATION SETUPS

In our study, we track a single bunch at a time (no coupled-bunch effects). The Gaussian and non-Gaussian bunches were used as the initial beam distributions at the low-energy

* Work supported by Institute of High Energy Physics.
† gywan@ihep.ac.cn

injection point of the booster for tracking. The Gaussian bunch features a Gaussian distribution with a 3σ cut-off in six-dimensional phase space. The non-Gaussian bunch is obtained from tracking simulations that incorporate linac and low-energy beam transport line errors along with corrections, yielding a distribution that is closer to the actual bunch. Table 2 shows the key parameters for these bunches at 300 MeV.

Table 2: Key Parameters of the Gaussian and Non-Gaussian Bunches at 300 MeV

Parameter	**Gaussian bunch**	**Non-Gaussian bunch**
Number of macroparticles	10000	10469
Bunch charge (nC)	8.5	8.5
Initial average energy (MeV)	299.49	303.02
Horizontal emittance (nm · rad)	125.68	134.94
Vertical emittance (nm · rad)	122.68	137.62
Energy spread (%)	0.78	1.17
Bunch length (mm)	2.92	1.57

The beam energy of these bunches was ramped from the initial average energy to 6 GeV in 0.4 s. Considering the requirements of the HEPS injector [7], we set a 0.2 s flat-bottom at the low-energy injection stage and a 0.2 s flat-top at the high-energy extraction stage in its energy variation curve. The RF voltage was adjusted accordingly along with the energy variation curve.

To ensure that these bunches are fully captured in the buckets during the simulations, we selected the initial RF voltages as shown in Fig. 1 for this study. Using an initial RF voltage of 2 MV as an example, Fig. 2 shows the corresponding variation curves of energy (blue) and RF voltage (red).

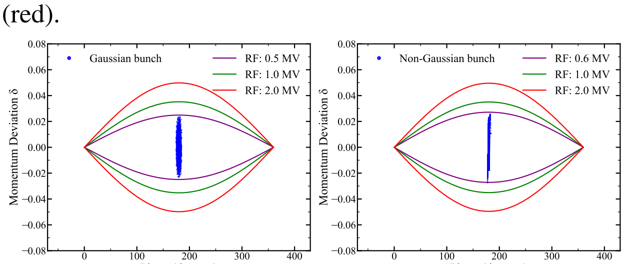

Figure 1: The Gaussian (left) and non-Gaussian (right) bunches within the buckets under different initial RF voltages.

SIMULATION RESULTS

Owing to the impedance spectrum, TMCI is more likely in the vertical [7, 8], so the horizontal chromaticity ξ_x is fixed

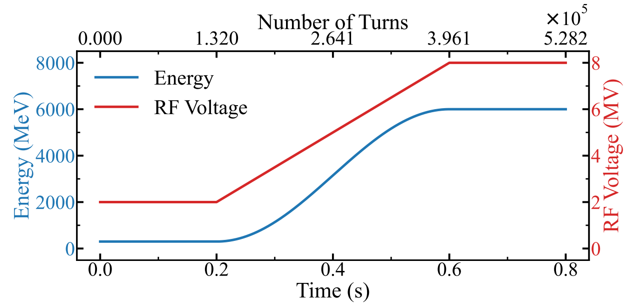

Figure 2: The variation curves of energy (blue) and RF voltage (red) with an initial voltage of 2 MV.

at 0.2. Following previous study at 500 MeV injection [7, 8], we adopt $\xi_y = 0.2$ as the baseline. At 300 MeV injection, the estimated TMCI threshold bunch charge is 7.8–9 nC under RF voltage 2 MV and $\xi_y = 0.2$ [2]. Since our bunch charge (8.5 nC) is close to this threshold, we also examine a higher $\xi_y = 0.7$ to potentially suppress TMCI [9]. Figure 3 shows the vertical oscillation of the bunch centroid (blue) and the beam transmission rate (red) over 10,000 turns under different conditions at 2 MV.

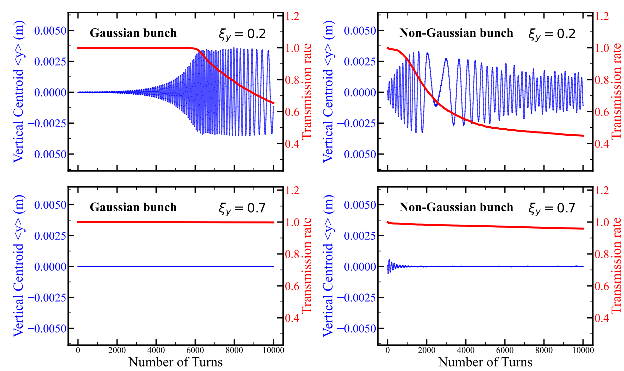

Figure 3: Simulation results for the Gaussian (left) and non-Gaussian (right) bunches under different vertical chromaticities when the initial RF voltage is set to 2 MV.

Figure 3 shows that when $\xi_y = 0.2$, the TMCI is triggered, leading to significant beam loss. In contrast, when $\xi_y = 0.7$, the TMCI is suppressed by the stronger Landau damping provided by the higher vertical chromaticity [9], only a minor amount of beam loss is observed. Table 3 presents the simulated beam transmission rates under different conditions.

Table 3: Beam Transmission Rates under Different Conditions

Initial RF voltage (MV)	**Gaussian**		**Non-Gaussian**	
	$\xi_y = 0.2$	$\xi_y = 0.7$	$\xi_y = 0.2$	$\xi_y = 0.7$
0.5	55.3%	98.4%	–	–
0.6	–	–	41.8%	89.3%
1.0	46.4%	96.7%	29.6%	83.1%
2.0	34.2%	93.3%	25.7%	70.2%

Table 3 shows that a lower initial RF voltage generally corresponds to a higher beam transmission rate, regardless of whether TMCI is triggered.

COMPARATIVE ANALYSIS

Simulation results comparing the Gaussian and non-Gaussian bunches show that even with the same chromaticity, charge, and initial RF voltage, there remains a significant difference in the beam transmission rates between these two cases. The beam transmission rates for the non-Gaussian bunch are consistently lower than that for the Gaussian bunch.

This difference likely arises from the distinct energy spreads of these bunches. The energy spread of the Gaussian bunch is 0.78%, which corresponds to a momentum deviation range of [-0.023, 0.024] for off-momentum particles. In contrast, the energy spread of the non-Gaussian bunch is 1.17%, which corresponds to a momentum deviation range of [-0.028, 0.025] for off-momentum particles.

To investigate the effects of off-momentum particles within the different momentum deviation ranges corresponding to the two bunches, we performed frequency map analysis for each case separately when setting the chromaticity to (0.2, 0.7). The results are shown in Fig. 4. As shown, the integer resonance at $\nu_x = 21$ is triggered when the momentum deviation range expands to [-0.028, 0.025]. Consequently, when the booster transmits the non-Gaussian bunch, larger off-momentum particles excite this resonance, causing particle loss and reducing the beam transmission rate.

It is assumed that the lost particles are all large off-momentum particles, we find that at the initial RF voltage of 2 MV, the fraction of particles with $|\delta| > 0.143$ is 6.7% for the Gaussian bunch and 29.1% for the non-Gaussian bunch. At 1 MV, the fraction of particles with $|\delta| > 0.164$ is 3.3% for the Gaussian bunch and 16.7% for the non-Gaussian bunch. These results are in excellent agreement with those in Table 3.

For the non-Gaussian bunch, shifting the working point to $\nu_x = 21.2$ mitigates the $\nu_x = 21$ resonance, increasing the beam transmission rate from 89.3% to 94.7% under initial RF voltage 0.6 MV and chromaticity (0.2,0.7).

Furthermore, this analysis points to the potential benefit of reducing the energy spread of the non-Gaussian bunch for improving the beam transmission rate. Therefore, using Eq. (1), we process the particle momentum distribution of the non-Gaussian bunch to systematically study the impact of different energy spread values (1.17%, 1.01%, 0.80%, all practically achievable in the HEPS injector) on the beam transmission rate.

$$p_{\text{new}} = p_{\text{avg}} + \alpha \cdot (p_{\text{old}} - p_{\text{avg}}) \qquad (1)$$

In Eq. (1), p_{avg} is the mean of the particle momentum distribution p_{old} of the original non-Gaussian bunch, α is the ratio of the target energy spread to the original energy spread, and p_{new} is the particle momentum distribution of a new non-Gaussian bunch obtained after the scaling process.

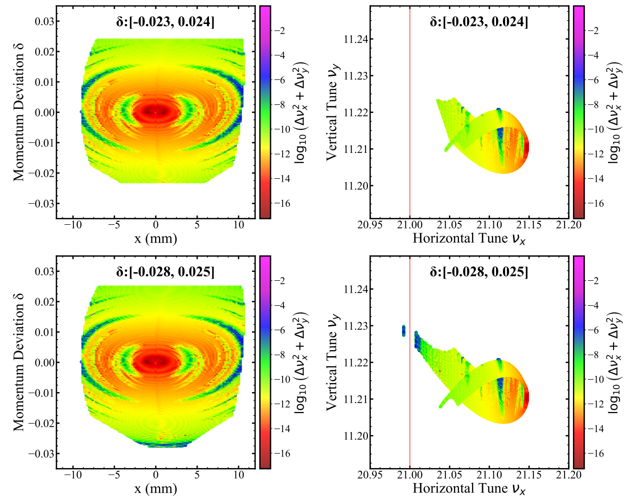

Figure 4: Frequency map analysis in the momentum space for off-momentum particles within different momentum deviation ranges when setting vertical position equal zero. Calculations are done at the injection location $\beta_x = 14.1$ m, $\beta_y = 15.4$ m. Diffusion maps (left) and tune $\nu_{x,y}$ footprint maps (right) for different initial horizontal offsets and off-momentum particles.

Through this data processing method, only the magnitude of the energy spread of the non-Gaussian bunch is altered.

In this simulations, the initial RF voltage is set to 0.6 MV, the chromaticity to (0.2, 0.7). Reducing the energy spread of the non-Gaussian bunch from 1.17% to 1.01% and 0.80% increases the beam transmission rate in the booster to 95.0% and 98.0%, respectively, from original ratio 89.3%.

DISCUSSION

For the Gaussian bunch, with an initial RF voltage of 0.5 MV and chromaticity of (0.2, 0.7), a charge of 8.4 nC/bunch can be transported in the booster, meeting the requirements of the HEPS. In contrast, the non-Gaussian bunch has a larger energy spread, which may cause some large off-momentum particles to trigger the integer resonance at $\nu_x = 21$. By reducing the energy spread to 0.80% of the non-Gaussian bunch under the initial RF voltage 0.6 MV and chromaticity (0.2, 0.7), a charge of 8.3 nC/bunch can be transported in the booster, also satisfying the HEPS operational requirements well.

Moreover, even when considering a realistic distribution of magnet errors and a 15% increase in the total impedance, a charge of 7.2 nC/bunch can still be transported, meeting the HEPS requirements and further reinforcing the robustness of our results.

CONCLUSION

Our results suggest that by optimizing the initial RF voltage, chromaticity, working point and the energy spread of the injected bunch, it is possible to achieve stable beam transport with a bunch charge exceeding 5 nC in the booster at the lower injection energy mode for the HEPS injector.

REFERENCES

[1] Y. M. Peng, *et al.*, “Design of the HEPS Booster Lattice”, *Radiation Detection Technology and Methods*, vol. 4, pp. 425-432, 2020.
doi:10.1007/s41605-020-00202-z

[2] J. Q. Wang, “Discussion on Further Performance Improvement of the HEPS Injector [In Chinese]”, work notes, Mar. 2025.

[3] G. Benedetti, *et al.*, “Commissioning of the ALBA Injector With 67 MeV Single Klystron Linac”, in *Proc. IPAC’16*, Busan, Korea, Jun. 2016, pp. 2905-2907.
doi:10.18429/JACoW-IPAC2016-WEPOW033

[4] X. Yang, *et al.*, "Operation of the NSLS-II Injector With a Lower Booster Injection Energy", *NSLS II TECHNICAL NOTE*, NSLSII-ASD-TN-253, Jul. 2017.
doi:10.2172/1504388

[5] X. Yang, *et al.*, "Development of New Operational Mode for NSLS-II Injector: Low-Energy 100 MeV Linac-to-Booster Injection", in *Proc. IPAC’18*, Vancouver, Canada, Jun. 2018, pp. 1330-1333.
doi:10.18429/JACoW-IPAC2018-TUPMF037

[6] M. S. Chiu, *et al.*, “Energy Ramping Simulation for TPS Booster Ring”, in *Proc. IPAC’25*, Taipei, Taiwan, Jun. 2025, pp. 2036-2039.
doi:10.18429/JACoW-IPAC2025-WEPM033

[7] Y. M. Peng and H. S. Xu, "Study of Single-Bunch Instability on Beam Transmission Rate during Low-Energy Injection and Energy Ramping in HEPS Booster Synchrotron [In Chinese]", *High Energy Photon Source Technical Notes*, HEPS-AC-AP-TN-2021-021-V0, Jul. 2021.

[8] H. S. Xu and N. Wang, "Collective Beam Instabilities in the HEPS Booster v3.0 Lattice [In Chinese]", *High Energy Photon Source Technical Notes*, HEPS-AC-AP-TN-2021-002-V0, Jan. 2021.

[9] H. S. Xu, Y. M. Peng and N. Wang, "Studies of Transverse Single-Bunch Instabilities in Booster Synchrotrons", *Nucl. Instrum. Methods Phys. Res. A*, vol. 940, pp. 313-319, 2019.
doi:10.1016/j.nima.2019.06.048